Acute mechanical performance of bioresorbable scaffolds compared with everolimus-eluting stents under optical coherence tomography guidance

Nagwa A. Abdelrahman[a,b], Arif A. Al Nooryani[a], Hatem A. Helmy[b], Yehia T. Kishk[b], Ayman K.M. Hassan[b]

[a]Cardiovascular Department, Al Qassimi Hospital, Sharjah, UAE, [b]Cardiovascular Department, Faculty of Medicine, Assiut University, Assiut, Egypt.

Correspondence to Nagwa A. Abdelrahman, MD, Department of Cardiovascular, Faculty of Medicine, Al-Orman Cardiology Hospital, Assiut University, Assiut 71515, Egypt.
Tel: +20 101 583 0156; Fax: +20 882 347 932; e-mail: nagwaabdelrahman@aun.edu.eg

Received 09 October 2019
Revised 08 November 2019
Accepted 21 November 2019
Published 16 May 2020

Journal of Current Medical Research and Practice
2020, 5:158–163

Objective
The aim was to compare the acute mechanical performance of the ABSORB bioresorbable scaffold (BRS) with the everolimus-eluted stents (EES) after optical coherence tomography (OCT)-guided deployment.

Background
The intrinsic differences in biomechanical properties between BRS and EES and the thicker BRS struts can affect the BRS acute mechanical performance in terms of scaffold expansion and struts apposition.

Materials and methods
The authors compared the acute mechanical performance of 245 scaffolds with that of 82 everolimus-eluted EES. All scaffolds/stents were deployed under OCT guidance. OCT was used to assess the following acute mechanical performance indices: residual area stenosis, device underexpansion, struts malapposition, edge dissection whether covered or uncovered, and strut fracture.

Results
Two hundred forty-five scaffolds implanted in 162 patients in the BRS arm were compared with 82 stents implanted in 61 patients in the EES arm. Final OCT acquisitions showed no statistically significant difference in the acute mechanical performance indices between both arms, in terms of residual area stenosis, device underexpansion, struts malapposition, and struts fracture. The only significant difference was noted in the higher rates of both covered and uncovered edge dissections in the BRS arm.

Conclusion
Under OCT guidance, there was no significant difference in the acute mechanical performance of BRS vs EES, apart from higher rates of both covered and uncovered edge dissections in the BRS arm.

Keywords:
bioresorbable scaffold, dissection, malapposition, optical coherence tomography

J Curr Med Res Pract 5:158–163

2357-0121

Introduction

Ideal stent deployment is critical during percutaneous coronary intervention (PCI), as residual stenosis and struts malapposition increase the risk of future in-stent restenosis and thrombosis [1,2].

Formerly, optimal stent implantation criteria were derived from intravascular ultrasound (IVUS)-based studies [3,4].

Edge dissection, struts malposition, and residual stenosis were found to be significant predictors of early stent thrombosis in an IVUS substudy of the Horizon AMI trial [5].

Bioabsorbable scaffolds (BRS) have emerged as a potential advance for treatment of coronary stenosis owing to the added advantage of complete bioresorption 2–3 years after implantation, with restoration of healthy endothelium, vascular pulsatility, and vasomotion [6,7].

The biomechanical properties, such as conformability and flexibility, substantially differ between BRS and metal stents resulting in different expansion patterns. The Absorb scaffold analysis revealed an eccentric expansion pattern compared with metallic stents, with subsequent higher rate of scaffold underexpansion and malapposition. The asymmetric expansion pattern of the radiolucent BRS is usually underestimated by

the conventional coronary angiography based on two-dimensional images [1,8].

It was crucial to confirm optimal scaffold implantation as underexpansion, and struts malapposition have been linked to the risk of scaffold thrombosis, the main reason for Absorb BRS setback and withdrawal [9,10].

In a subanalysis of the Absorb Cohort B trial, acute scaffold fractures and serious struts malapposition were not detected at all by conventional angiography, whereas only partly detected by IVUS, but fully detected with the optical coherence tomography (OCT) [11].

OCT is a promising light-based high-resolution intracoronary imaging modality that allows accurate detection and quantification of scaffold characteristics [1].

Recently, the 2018 ESC/EACTS guidelines on myocardial revascularization highlight the OCT importance owing to its accuracy in the assessment of mechanical performance indices such expansion pattern, residual stenosis, struts malapposition, and edge dissection [12].

Our aim was to compare the acute mechanical performance of the ABSORB BRS with the everolimus-eluting stents (EES) under OCT-guided deployment.

Materials and methods

Study design and population

We performed an observational study comparing Absorb BRS with EES in all patients who had OCT-guided PCI at Al Qassimi Hospital, Sharjah, UAE, from March 2013 to October 2017.

All patients provided signed informed consent for scaffold/stent deployment and OCT guidance at the time of the procedure.

The devices included in the EES group were the everolimus-eluting Xience Xpedition, Prime and Alpine stents (Abbott Vascular, Santa Clara CA, USA), and Promus Element and Premiere stents (Boston Scientific, Natick, Massachusetts, USA).

The protocol complied with Helsinki declaration and was approved by both Sharjah Medical District Research Ethics Committee, IRB: MOHAP/SHJ1412017, and Assiut University Hospitals (homeland of the co-authors), IRB: 17200359.

Owing to the retrospective, observational nature of the study, waiver of the informed consent was agreed upon, provided confidentiality of the patients' identities.

Procedures

Patients were pretreated with either clopidogrel 600 mg or ticagrelor 180 mg and aspirin 300 mg as required.

Initial predilatation was performed in most lesions. Unlike for EES, BRS implantation was performed using slowly progressive balloon inflation (i.e. 1 atm/5 s). Postdilatation was undertaken in case of scaffold/stent underexpansion or struts malapposition until optimal deployment was achieved according to OCT findings.

Optical coherence tomography performance

OCT was performed using either the ILUMIEN OPTIS PCI Optimization System (St. Jude Medical, St. Paul, Minnesota, USA) or the LUNAWAVE OCT System (Terumo, Japan).

The OCT catheter was inserted distal to the scaffold/stent, and automatic pullbacks were performed at 20 mm/s during injection of iso-osmolar iodixanol (Visipaque; GE Healthcare, Little Chalfont, Buckinghamshire, UK) to limit artefacts from blood.

The pullback was performed until reaching the maximal pullback length (7.4 cm with the Ilumien Optis system and 10 cm with the LUNAWAVE OCT System, ILUMIEN OPTIS PCI Optimization System with the Dragonfly-Duo intracoronary imaging catheter [both St. Jude Medical, St. Paul, MN, USA]). Two consecutive pullbacks were performed when required.

Off-line optical coherence tomography analysis

Complete analysis at 2 mm interval was conducted for the whole stented segment plus 4 mm segments distal as well as proximal to the scaffold/stent. Proximal and distal segments were examined to calculate the reference vessel area (RVA) and to detect dissections.

Acute mechanical performance was assessed using the following indices: residual area stenosis (RAS), underexpansion, incomplete strut apposition (ISA), strut fracture, and edge dissection.

The percentage of RAS was calculated as follows: [1–(minimal lumen area/RVA)]×100. RVA is the mean of the two largest luminal areas within 4 mm proximal and distal to the scaffold/stent edge[13] (Fig. 1). In case of ostial lesion or the presence of a large side branch at the stent edge, rendering a

Figure 1

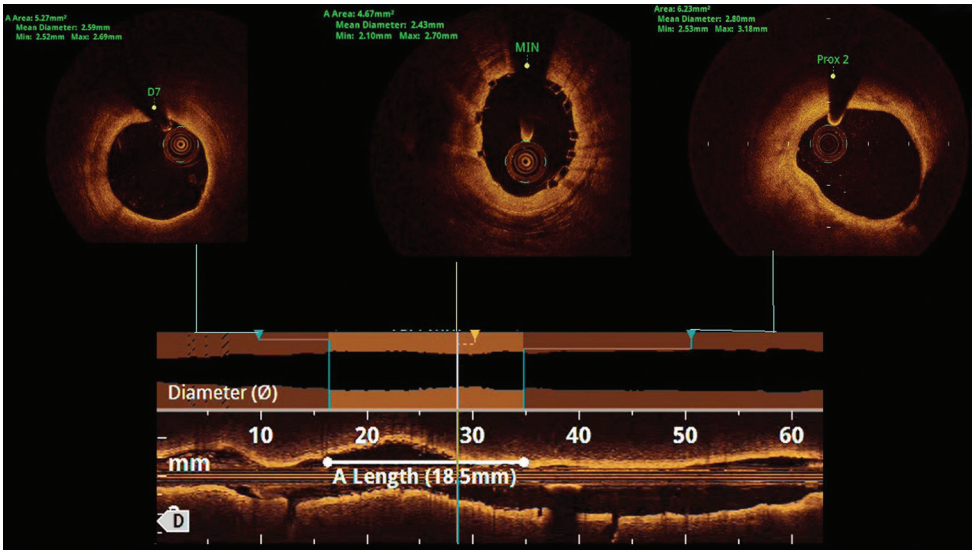

Optical coherence tomography longitudinal section showing an example of residual area stenosis calculation. Reference vessel area is the mean of the proximal (Pro × 2) and distal (D7) segments lumen area; reference vessel area = 6.23 + 5.27/2 = 5.75 mm^2. Residual area stenosis =[1−(minimal lumen area/reference vessel area)]×100=[1−(4.67/5.75 mm^2)]×100 = 19%.

meaningful proximal or distal segment unfeasible, only a proximal or distal reference cross-section was used to calculate the RVA [14].

Scaffold/stent underexpansion was defined as a RAS greater than 30%. Stent fracture was assumed in case of interruption of the device circularity, superseding struts, and isolated malapposed struts in the lumen[13] (Fig. 2).

Edge dissection was demarcated as intimal disruption at the stent edge with a flap (Fig. 3a). Polymeric BRS struts appear in OCT as black boxes without abluminal shadowing, thus BRS strut malapposition was identified in case of strut separation from the luminal wall (Fig. 3b). This was not the same in case of metallic struts which induce backward reflection and shadowing on OCT, for which malapposition was considered when the distance between the strut's surface and the luminal wall is more than the strut thickness (90 μm) [13,15] (Fig. 3c). The malapposed struts percentage was calculated as follows: total number of malapposed struts observed at 2mm intervals/struts total number × 100 [16].

Statistical analysis

Data analysis were done using SPSS version 19 (Statistical Package for the Social Sciences, IBM Corp., Armonk, N.Y., USA). Descriptive statistics (means and SDs for continuous variables with normal distribution and frequency for categorical variables) were computed according to treatment type (BRS or EES).

Comparison between groups for continuous variables was performed by the Mann–Whitney *U*-test (in case of nonparametric distribution).

Significance of associations was assessed using the χ^2-test or the Fisher exact test, as appropriate. For all the statistical tests used, a *P* value less than 0.05 was considered statistically significant.

Results

Population

Two hundred forty-five scaffolds implanted in 162 patients in the BRS arm (75% males, mean age 53.5 ± 26 years) were compared with 82 stents implanted in 61 patients in the EES arm (77% males, mean age 51 ± 25 years).

There was no significant difference in the patients' baseline characteristics between both groups. Overall, 64 and 57.4% of the patients had a history of hypertension (*P* = 0.349), 74.1 and 75.4% had dyslipidemia (*P* = 0.838), 57.4 and 67.2% had diabetes mellitus (*P* = 0.183), whereas 36.5 and 37.7% were current smokers (*P* = 0.873) in the BRS and EES arms, respectively.

Overall, 12 and 11.5% of patients presented with silent ischemia (*P* = 0.958), 30.8 and 34.4% with stable angina (*P* = 0.611), 38.8 and 45.9% with acute coronary syndrome (*P* = 0.342), and 18.4 and 8.2% with STEMI (*P* = 0.058), in the BRS and EES arms, respectively.

Procedural characteristics

The procedures were performed via the radial approach in 107 (66%) and 35 (57%) patients for BRS and

Figure 2

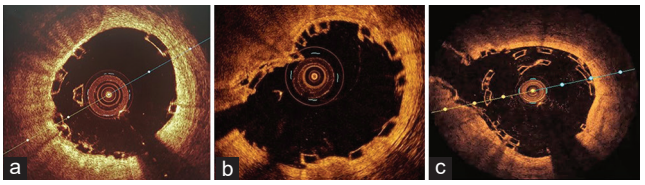

Optical coherence tomography pictures of struts fracture in the form of isolated malapposed struts inside the lumen (a), interruption of the device circularity (b), and superseded struts (c).

Figure 3

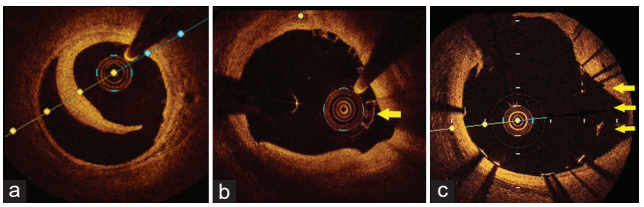

Optical coherence tomography images of (a) edge dissection showing the intimal disruption with intimal flap, (b) incomplete strut apposition of bioresorbable scaffold scaffold, where struts are clearly separated from the luminal wall (arrow), (c) incomplete strut apposition of metallic struts axial distance greater than 90 μm (three arrows).

EES, respectively (P = 0.229), and the rest of the patients through the femoral approach using standard techniques.

Xience Xpedition EES was the most frequently used EES [68 (83%)], whereas Xience Prime, Xience Alpine, and Promus Element and Premiere EES were used in seven (8.5%), three (3.5%), and four (5%) of cases, respectively.

The left anterior descending artery (LAD) was the target vessel in a large proportion of cases in both groups (BRS, 55.9%; EES, 61.5%; P = 0.428). Left main artery was the target in 2.2 and 23.1% (P = 0.001), left circumflex artery in 19.6 and 18.4% (P = 0.863), right coronary artery in 24.0 and 15.4% (P = 0.148), and saphenous venous grafts in 0.6 and 1.5% (P = 0.463) in the BRS and EES arms, respectively.

A range of lesion morphologies were included in the study, with 5.0 and 1.5% type A lesions (P = 0.297), 30.2 and 27.7% type B1 lesions (P = 0.708), 29.6 and 40.0% type B2 lesions (P = 0.125), and 35.2 and 30.8% type C lesions (P = 0.509) in the BRS and EES arms, respectively.

Lesions included chronic total occlusions (4.5 vs 3.7%; P = 0.747), bifurcations (7.3 vs 20.7%; P = 457), and ostial lesions (16.3 vs 42.7%; P < 0.001) in the BRS and EES arms, respectively.

The overall predilatation rate was significantly higher in the BRS arm than the EES arm, with 231 (94.3%) and 71 (86%), respectively (P = 0.023). NC balloons were more frequently used for lesion preparation in the BRS arm (BRS, 65.7%; EES, 45%; P = 0.001). A higher balloon/device diameter ratio was used for predilatation in the BRS arm (BRS, 0.96 ± 0.11; EES, 0.90 ± 0.13; P < 0.001). However, this difference is mainly owing to the different techniques of implantation as advised by the manufacturer, and was done on purpose; thus, it does not reflect an effect of OCT use.

A higher balloon/device diameter ratio was used for postdilatation in the BRS arm (BRS, 1.10 ± 0.09; EES, 1.08 ± 0.12; P = 0.025), with significantly higher inflation time and pressure for postdilatation in the BRS arm compared with EES arm (15.88 ± 6.22; vs 13.7 ± 3.44 s, P = 0.004 and 17.89 ± 4.04 vs 16.84 ± 4.03 atm, P = 0.028, respectively).

Sizes of the BRS scaffolds used were 3.0 ± 0.5 mm in diameter and 8, 12, 18, 23, 25, and 28 mm in length, whereas EES sizes were 3.0 ± 1.0 mm in diameter and 8, 15, 18, 20, 23, 24, 28, 33, 38, and 48 mm in length. Table 1 demonstrates the percentages of scaffold/stent diameter used in each arm.

Optical coherence tomography findings

OCT findings are illustrated in Table 2. A total of 6568°CT frames and 43 201 struts were studied.

Final OCT acquisitions after modifications showed no statistically significant difference in the acute mechanical performance indices between both arms, in terms of RAS, device underexpansion, struts malapposition, and struts fracture. The only significant difference was noted in the higher rates of both covered and uncovered edge dissections in the BRS arm.

Strut fractures were not detected in the EES arm, but spotted in four scaffolds, three of them were owing to postdilatation at high pressure against rings of heavy calcification and calcium spikes (Fig. 2a, b), but one scaffold showed struts fracture after bifurcation stenting using culotte technique (Fig. 2c).

In-hospital course

OCT imaging was not associated with any complication in the studied population.

There was no significant difference between both arms in the rate of in-hospital events. A case of subclavian artery dissection by the guiding catheter was reported in the BRS arm, for which computed tomography (CT) with contrast to the subclavian artery was performed. The case was managed conservatively with follow-up

CT after 1 week and 1 month. Intra-aortic balloon pump was required during primary PCI in one patient with low ejection fraction (33%) in the BRS arm. Acute in-hospital course and complications are summarized in Table 3.

Discussion

Thick polymer-based BRS have different mechanical properties than thin second-generation EES [16].

Tateishi *et al.*[17] defined standards for an optimal BRS implantation as not only absence of malapposition but also perfect embedment of the struts into the vessel wall, thus avoiding laminar flow disturbance by the protruding struts.

In the present study, we implemented a standardized methodology of OCT measurement that enables fair evaluation of BRS vs EES, considering the intrinsic difference between both devices such as the translucency of the poly-l-lactic acid scaffolds, the thicker BRS struts, and the BRS asymmetric expansion pattern [18].

Table 1 Frequency of used devices diameters

Device diameter (mm)	BRS (*n*=245) [*n* (%)]	EES (*n*=82) [*n* (%)]	*P*
2.25	0	2 (2.4)	0.014
2.5-2.75	44 (18.0)	17 (20.7)	0.576
3.0	85 (34.7)	19 (23.2)	0.052
3.5-4.0	116 (47.3)	44 (53.7)	0.322

BRS, bioresorbable scaffold; EES, everolimus-eluting stent.

Table 2 Optical coherence tomography findings

Number of stents	BRS (*n*=245)	EES (*n*=82)	*P*
Malapposing struts			
Mean±SD	3.34±4.27	3.89±4.30	0.250
Median (range)	2.1 (0.0-25.0)	2.8 (0.0-24.0)	
Fractured scaffold/stent	4 (1.6)	0	0.576
Under-expansion	27 (11.0)	10 (12.2)	0.771
Residual area stenosis			
Mean±SD	14.31±12.98	15.59±14.78	0.677
Median (range)	12.0 (0.0-65.0)	13.5 (0.0-51.0)	
Edge dissection [*n* (%)]			
Covered dissection	16 (6.5)	1 (1.2)	0.013
Uncovered dissection	37 (15.1)	5 (6.1)	

BRS, bioresorbable scaffold; EES, everolimus-eluting stent.

Table 3 In hospital events and complications

In hospital events	BRS (*n*=162) [*n* (%)]	EES (*n*=61) [*n* (%)]	*P*
Smooth course	158 (97.5)	59 (96.7)	0.666
Femoral hematoma	1 (0.6)	1 (1.6)	0.473
IABP	1 (0.6)	0	0.538
Subclavian artery injury	1 (0.6)	0	0.538
Heart failure	0	1 (1.6)	0.274

BRS, bioresorbable scaffold; EES, everolimus-eluting stent; IABP, intra-aortic balloon pump.

Our OCT image analysis showed that there was no significant difference in the acute mechanical performance of BRS vs EES in terms of incomplete struts apposition, scaffold/stent underexpansion, and RAS.

We reported a mean percentage of ISA of 3.34 ± 4.27 and 3.89 ± 4.30% in Absorb BRS and EES, respectively (P = 0.250), both are lower than the 5% identified as a criterion for non-optimal BRS deployment [14].

However, the edge dissection rate was significantly higher in the BRS arm compared with the EES arm (21.6 vs 7.3%, respectively). This can be explained by the higher postdilatation balloon/device diameter ratio, inflation time, and pressure during Absorb BRS deployment. Another explanation can be the sharp borders of the Absorb struts dissecting the vascular intima during implantation.

Our findings are in concordance with the results of Mattesini *et al.* [16], who suggested that appropriate lesion preparation and OCT-guided implantation can achieve a satisfactory BRS expansion in complex coronary lesions, thus alleviating the impression that acute performance of BRS is always inferior to metallic EES [19].

The BRS edge dissection rate in the current study (21.6%) was higher than that reported by Mattesini and colleagues (7.9%), but lower than the 35% spotted in the cohort B trial for which no explanation could be found [14,16].

The OCT detected acute scaffold fracture in the current study was 1.6%, lower than the 3.9% spotted by the OCT analysis of the Absorb cohort B trial. Scaffold fractures in the cohort B trial were attributed only to the extreme scaffold overexpansion beyond the predetermined manufacturer limits; however, this was not the only explanation in our study. Bifurcation stenting using the culotte technique was defined as a culprit for scaffold fracture, proved by the overriding struts after culotte stenting. Another discovered reason of fracture was the severe calcification hindering proper expansion particularly in the presence of calcium spikes, thus, highlighting the importance of presenting OCT for lesion selection.

We reported a lower mean percentage of ISA in the BRS arm compared with Absorb Cohort B study (3.34 vs 6.2%), as well as a lower RAS (14.31 ± 12.98 vs 21.6 ± 15.9). These differences can be explained by the more frequent postdilatation in the studied population (96.7%) vs only 60% in the Cohort B study [14].

Study limitations

It is a single-center observational study that requires confirmation in larger multicenter trials.

Conclusion

Under OCT guidance, there was no significant difference in the acute mechanical performance of BRS vs EES, apart from higher rates of both covered and uncovered edge dissections in the BRS arm.

Financial support and sponsorship

Nil.

Conflicts of interest

There are no conflicts of interest.

References

1 Allahwala UK, Cockburn JA, Shaw E, Figtree GA, Hansen PS, Bhindi R. Clinical utility of optical coherence tomography (OCT) in the optimisation of Absorb bioresorbable vascular scaffold deployment during percutaneous coronary intervention. Eurointervention 2015; 10:1154–1159.

2 Palmerini T, Biondi-Zoccai G, Della Riva D, Stettler C, Sangiorgi D, D'Ascenzo F, *et al*. Stent thrombosis with drug-eluting and bare-metal stents: evidence from a comprehensive network meta-analysis. Lancet 2012; 379:1393–1402.

3 Sonoda S, Morino Y, Ako J, Terashima M, Hassan AH, Bonneau HN, *et al*. Impact of final stent dimensions on long-term results following sirolimus-eluting stent implantation: serial intravascular ultrasound analysis from the Sirius trial. J Am Coll Cardiol 2004; 43:1959–1963.

4 Costa MA, Angiolillo DJ, Tannenbaum M, Driesman M, Chu A, Patterson J, *et al*. Impact of stent deployment procedural factors on long-term effectiveness and safety of sirolimus-eluting stents (final results of the multicenter prospective STLLR trial). Am J Cardiol 2008; 101:1704–1711.

5 Vlachojannis GJ, Claessen BE, Dangas GD. Early stent thrombosis after percutaneous coronary intervention for acute myocardial infarction. Interv Cardiol 2012; 7:33–36.

6 Lesiak M, Araszkiewicz A. 'Leaving nothing behind': is the bioresorbable vascular scaffold a new hope for patients with coronary artery disease? Postep Kardiol Inter 2014; 10: 283–288.

7 Serruys PW, Onuma Y, Ormiston JA, de Bruyne B, Regar E, Dudek D, *et al*. Evaluation of the second generation of a bioresorbable everolimus drug-eluting vascular scaffold for treatment of de novo coronary artery stenosis: six-month clinical and imaging outcomes. Circulation 2010; 122:2301–2312.

8 Zhang YJ, Bourantas CV, Muramatsu T, Iqbal J, Farooq V, Diletti R, *et al*. Comparison of acute gain and late lumen loss after PCI with bioresorbable vascular scaffolds vs everolimus-eluting stents: an exploratory observational study prior to a randomised trial. Eurointervention 2014; 10:672–680.

9 Hassan AK, Bergheanu SC, Stijnen T, van der Hoeven BL, Snoep JD, Plevier JW, *et al*. Latestent malapposition risk is higher after drug-eluting stent compared with bare-metal stent implantation and associates with late stent thrombosis. Eur Heart J 2010;31:1172–1180.

10 Forrestal BJ, Lipinski MJ. Bioresorbable scaffolds: fading away or hope for the future? JACC 2018. Available from: https://www.acc.org/latest-in-cardiology/articles/2018/02/07/07/45/bioresorbable-scaffolds. [Last accessed on 2018 Feb 07].

11 Onuma Y, Serruys P, Muramatsu T, Nakatani SH, Geuns RJ, B de Bruyne, Dudek D. Incidence and imaging outcomes of acute scaffold disruption and late structural discontinuity after implantation of the absorb everolimus-eluting fully bioresorbable vascular scaffold. Optical Coherence Tomography Assessment in the ABSORB Cohort B Trial. JACC Cardiovas Interv 2014; 7:1400–1411.

12 The Task Force on myocardial revascularization of the European Society of Cardiology (ESC) and European Association for Cardio-Thoracic Surgery (EACTS). 2018 ESC/EACTS Guidelines on myocardial revascularization. Eur Heart J 2018; 00:1–96,

13 Tearney GJ, Regar E, Akasaka T, Adriaenssens T, Barlis P, Bezerra HG, *et al*. Consensus standards for acquisition, measurement, and reporting of intravascular optical coherence tomography studies: a report from the International Working Group for Intravascular Optical Coherence Tomography Standardization and Validation. J Am Coll Cardiol 2012; 59:1058–1072.

14 Gomez-Lara J, Diletti R, Brugaletta S, Onuma Y, Farooq V, Thuesen L, *et al*. Angiographic maximal luminal diameter and appropriate deployment of the everolimus-eluting Bioresorbable vascular scaffold as assessed by optical coherence tomography: an ABSORB cohort B trial sub-study. EuroIntervention 2012; 8:214–224.

15 Serruys PW, Onuma Y, Dudek D, Smits PC, Koolen J, Chevalier B. Evaluation of the second generation of a bioresorbable everolimus-eluting vascular scaffold for the treatment of de novo coronary artery stenosis: 12-month clinical and imaging outcomes. J Am Coll Cardiol 2011; 58:1578–1588.

16 Mattesini A, Secco GG, Dall'Ara G, Ghione M, Rama-Merchan JC, Lupi A, *et al*. ABSORB biodegradable stents versus second-generation metal stents. A comparison study of 100 complex lesions treated under OCT guidance. JACC 2014; 7:741–750.

17 Tateishi H, Suwannasom P, Sotomi Y, Nakatani S, Ishibashi Y, Tenekecioglu E, *et al*. Investigators of the ABSORB cohort b study. Edge vascular response after resorption of the everolimus-eluting bioresorbable vascular scaffold – a 5-year serial optical coherence tomography study. Circ J 2016; 80:1131–1141.

18 Nakatani SH, Sotomi Y, Ishibashi Y, Grundeken MJ, Tateishi H, Tenekecioglu E, *et al*. Comparative analysis method of permanent metallic stents (XIENCE) and bioresorbable poly-L-lactic (PLLA) scaffolds (Absorb) on optical coherence tomography at baseline and follow-up. Eurointervention 2016; 12:1498–1509.

19 Kimura T, Kozuma K, Tanabe K, Nakamura S, Yamane M, Muramatsu T. A randomized trial evaluating everolimus-eluting Absorb bioresorbable scaffolds vs everolimus-eluting metallic stents in patients with coronary artery disease: ABSORB Japan. Eur Heart J 2015; 36:3332–3342.